Computational Quantum Physics & Applications:
Shannon Entropy and Information Content in Restricted Hartree-Fock Atomic Densities (Z = 2–10)

ELEFTHERIOS MARIOS ZOGRAFOS
AEM: 4428

## Introduction

Information-theoretic tools offer a powerful lens for quantifying the complexity and uncertainty inherent in quantum systems. Central to this framework are information-theoretic measures such as the Shannon entropy, which provides a basis-independent measure of how delocalized a particle's wavefunction is, far beyond what simple variances or expectation values can capture [1]. Complementary metrics and divergence measures have been introduced to probe other facets of a quantum density's shape and its deviation from idealized models.

In this study, we apply this suite of information measures to the second-period atoms (He through Ne), using Restricted Hartree–Fock (RHF) wavefunctions expanded in Slater-type orbitals[2].

## Objectives

The specific goals of this study are to:

1. Compute the coordinate-space Shannon entropy $S_r$ and momentum-space entropy $S_k$ for each element $Z = 2$–$10$ in its RHF ground state.

2. Evaluate the maximum-entropy bound $S_{\max}$, the Fisher information $I$, the Onicescu information energy inverse $O$ and the order parameter $\Omega$.

3. Construct two reference radial densities:

   (a) A hydrogenic 1s density determined by the first ionization potential.

   (b) The Thomas–Fermi statistical density for atomic charge $Z$.

4. Quantify the deviation of the RHF densities from each reference model using symmetrized Kullback–Leibler and Jensen–Shannon divergences.

## Theory

### RHF Radial Expansion

In the Roothaan–Hartree–Fock approach, each spin-independent radial orbital $R_{n\ell}(r)$ is expanded in a finite sum of primitive Slater-type functions:

$$R_{n\ell}(r) = \sum_j C_{jn\ell}\, S_{j\ell}(r),$$

where the normalized primitive basis functions are

$$S_{j\ell}(r) = N_{j\ell}\, r^{\,n_{j\ell}-1}\, e^{-Z_{j\ell}\, r},$$

and the normalization constants $N_{j\ell}$ are

$$N_{j\ell} = \frac{(2Z_{j\ell})^{\,n_{j\ell}+\frac{1}{2}}}{\sqrt{(2n_{j\ell})!}}\,.$$

Here $n_{j\ell}$ is the principal quantum number of the primitive, $Z_{j\ell}$ its exponent, and $C_{jn\ell}$ the self-consistent RHF expansion coefficients [2].

### Momentum-Space Radial Wavefunctions

The corresponding radial wavefunction in momentum space, $\widetilde{R}_{n\ell}(k)$, is related to $R_{n\ell}(r)$ by a spherical Bessel transform:

$$\widetilde{R}_{n\ell}(k) = 4\pi \int_0^\infty r^2\, R_{n\ell}(r)\; j_\ell(k\, r)\, dr,$$

where $j_\ell(k\, r)$ is the spherical Bessel function of order $\ell$. This transform ensures the normalization $\int_0^\infty |\widetilde{R}_{n\ell}(k)|^2\, k^2\, dk = 1$ whenever $\int_0^\infty |R_{n\ell}(r)|^2\, r^2\, dr = 1$.

### Shannon Entropy and Related Measures

Given the normalized radial probability density in coordinate space,

$$p_r(r) \;=\; \frac{1}{4\pi} \sum_{i=1}^{N_e} \bigl|R_i(r)\bigr|^2, \qquad \int_0^\infty p_r(r)\, 4\pi r^2\, dr = 1\,,$$

the coordinate-space Shannon entropy is[3]

$$S_r = -4\pi \int_0^\infty p_r(r)\; \ln p_r(r)\; r^2\, dr$$

Similarly, the momentum-space density $p_k(k)$ (obtained via Fourier/Bessel transform of $R_i(r)$) yields

$$S_k = -4\pi \int_0^\infty p_k(k)\; \ln p_k(k)\; k^2\, dk^{[3]}$$

The upper limit is defined

$$S_{\max} = 3\bigl(1 + \ln \pi\bigr) \;+\; \frac{3}{2}\, \ln\!\Bigl(\frac{4}{9}\, \langle r^2\rangle\, \langle k^2\rangle\Bigr)\,,$$

$$\langle r^2 \rangle = 4\pi \int_0^\infty p_r(r)\, r^4\, dr, \qquad \langle k^2 \rangle = 4\pi \int_0^\infty p_k(k)\, k^4\, dk.$$

Other information measures include:

- **Fisher information:**

$$I = 4\pi \int_0^\infty \frac{\big(p_r'(r)\big)^2}{p_r(r)}\, r^2\, dr,$$

which quantifies the "sharpness" of the density via its local gradients.

- **Onicescu's information energy:**

For a three-dimensional spherically-symmetric atomic density $p_r(r)$ in coordinate space and its momentum-space analogue $p_k(k)$, these generalize to

$$E_r = \int_0^\infty p_r(r)^2\, 4\pi\, r^2\, dr, \quad E_k = \int_0^\infty p_k(k)^2\, 4\pi\, k^2\, dk.$$

To obtain a single measure of information concentration that spans both spaces, we therefore define [3]

$$O = \frac{1}{E_r\, E_k}$$

which decreases as the overall density becomes more delocalized and increases as the electron density becomes more tightly concentrated.

- **Order parameter:** Following Landsberg's approach. Let

$$S \;=\; S_r + S_k$$

be the total Shannon entropy of the system and $S_{\max}$ its maximum allowed value. Then the order parameter is defined as [3]

$$\Omega = 1 \;-\; \frac{S}{S_{\max}}$$

By construction, $0 \le \Omega \le 1$, with $\Omega = 1$ indicating a perfectly "ordered" state and $\Omega = 0$ corresponding to complete disorder.

## Divergence Measures

To compare an density $p$ against a reference density $q$, we employ:

### Symmetrized Kullback–Leibler divergence

$$SK(p,q) = \int \Big[p(r)\ln\frac{p(r)}{q(r)} + q(r)\ln\frac{q(r)}{p(r)}\Big]\, dr,$$

### Jensen–Shannon divergence

$$JS(p,q) = H\big(\tfrac{p+q}{2}\big) - \tfrac{1}{2}H(p) - \tfrac{1}{2}H(q),$$

with Shannon entropy functional

$$H(r) = -\int r(x)\, \ln r(x)\, d\tau.$$

The Jensen–Shannon divergence is symmetric, bounded ($0 \le JS \le \ln 2$), and defines a true metric on the space of probability densities [3].

# Results

## Shannon Entropies & Information Measures

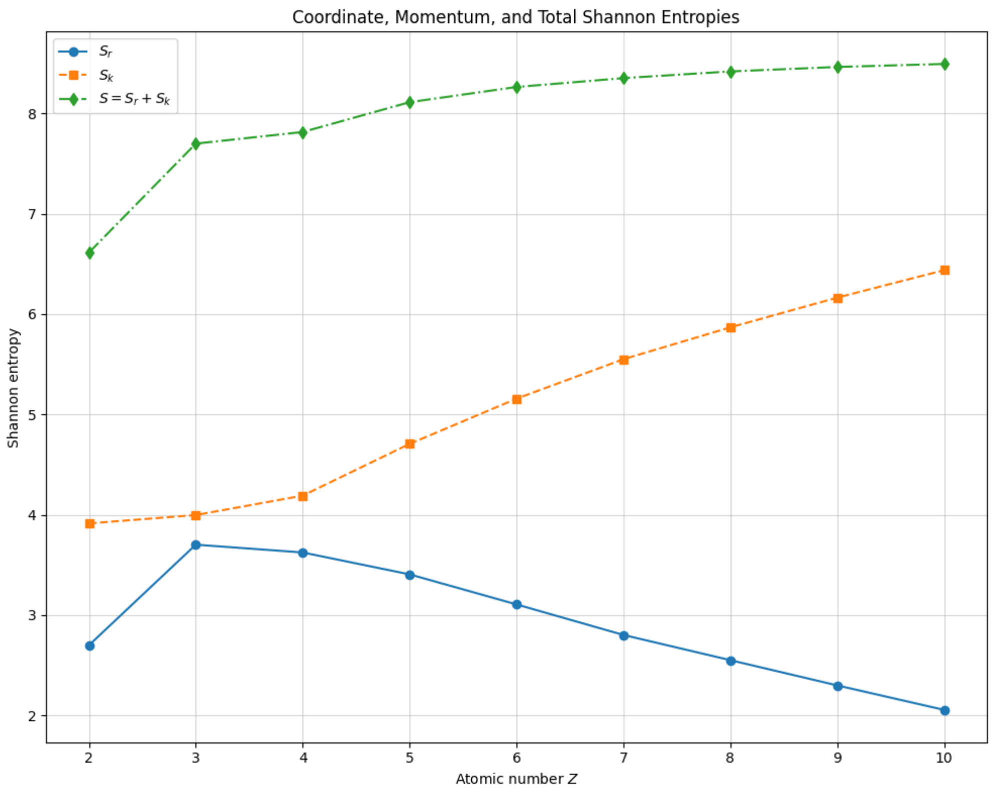


Figure 1: Coordinate-space entropy $S_r$ (blue circles), momentum-space entropy $S_k$ (orange squares), and total entropy $S = S_r + S_k$ (green diamonds) as functions of atomic number $Z$.

Figure 1 shows how the coordinate-space entropy $S_r$, momentum-space entropy $S_k$, and their sum $S = S_r + S_k$ evolve across the second-period atoms. As $Z$ increases from He to Ne, $S_r$ decreases monotonically, reflecting the fact that the electrons become more tightly bound (more localized near the nucleus). Conversely, $S_k$ increases steadily, indicating greater spread in momentum space as the wavefunctions sharpen in $r$-space. The total entropy $S$ thus grows slowly with $Z$, illustrating the entropic uncertainty trade-off between position and momentum.

Figure 2 shows:

(a) **Fisher information $I$:** Increases rapidly with $Z$

(b) **Onicescu measure $O$:** Drops steeply from He to a minimum near B/Be and then grows steadily for higher $Z$.

(c) **Order parameter $\Omega$:** Peaks at Li ($Z = 3$) and then decreases as the total entropy $S$ approaches its maximum bound less rapidly in heavier atoms.

(d) **Entropy bound $S_{\max}$:** Rises from He to a maximum around Be/B, then decreases gradually for larger $Z$, mirroring the combined variance in $r$- and $k$-space.

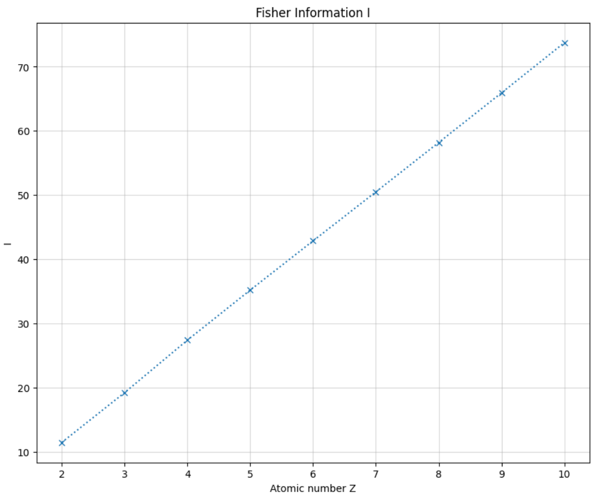


(a) Fisher information $I$.

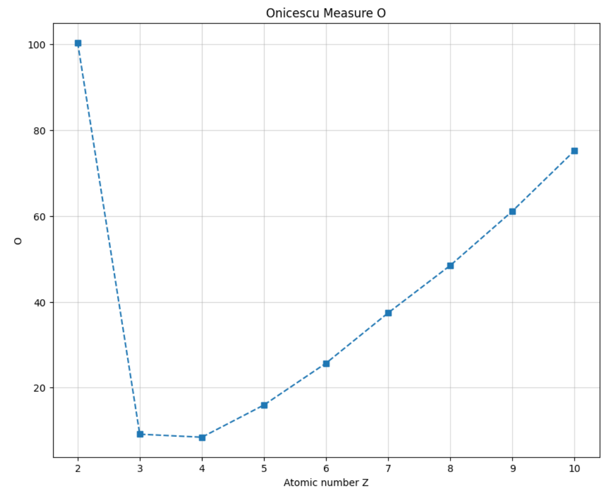


(b) Onicescu measure $O$.

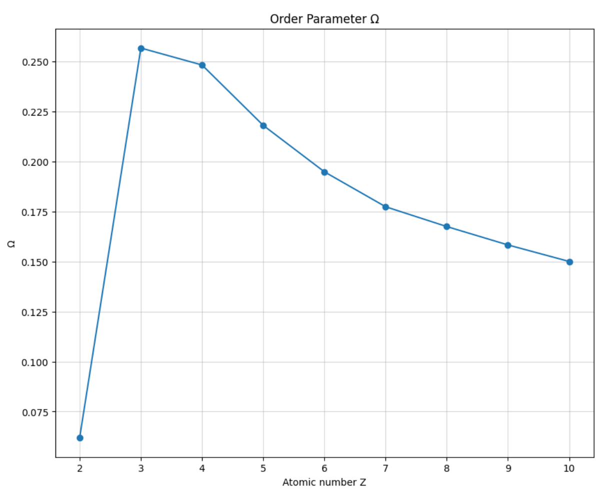


(c) Order parameter $\Omega$.

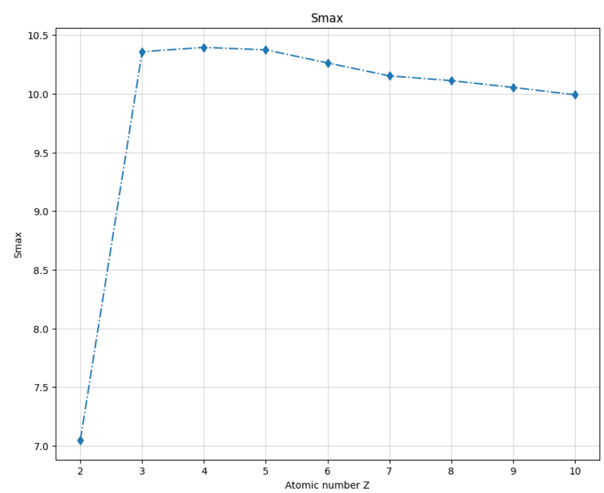


(d) Entropy bound $S_{\max}$.

Figure 2: (a) Fisher information, (b) Onicescu measure, (c) order parameter, and (d) entropic bound as functions of $Z$.

Table 1: Information measures for second-period atoms (He–Ne).

| $Z$ | $S_r$ | $S_k$ | $S$ | $S_{\max}$ | $O$ | $I$ | $\Omega$ |
|---|---|---|---|---|---|---|---|
| 2 | 2.698508 | 3.913415 | 6.611923 | 7.049306 | 100.361884 | 11.454178 | 0.062046 |
| 3 | 3.701437 | 3.996822 | 7.698259 | 10.357876 | 9.157066 | 19.215893 | 0.256772 |
| 4 | 3.623855 | 4.190193 | 7.814047 | 10.395109 | 8.454199 | 27.401481 | 0.248296 |
| 5 | 3.405437 | 4.705913 | 8.111350 | 10.373994 | 15.964618 | 35.197331 | 0.218107 |
| 6 | 3.106013 | 5.156601 | 8.262614 | 10.262665 | 25.709658 | 42.863441 | 0.194886 |
| 7 | 2.801667 | 5.549377 | 8.351044 | 10.152339 | 37.425422 | 50.495983 | 0.177427 |
| 8 | 2.550506 | 5.867411 | 8.417917 | 10.111782 | 48.469644 | 58.190730 | 0.167514 |
| 9 | 2.298780 | 6.163409 | 8.462190 | 10.053962 | 61.117092 | 65.928619 | 0.158323 |
| 10 | 2.055072 | 6.437178 | 8.492251 | 9.991642 | 75.194302 | 73.749726 | 0.150065 |

## Information-theoretic Divergences

Figures 3a–3b and 3c–3d chart the symmetrized Kullback–Leibler (KL) and Jensen–Shannon (JS) divergences against two reference densities:

Both hydrogenic- and Thomas–Fermi reference models yield *low* JS divergences ($\lesssim 0.2$), indicating that simple one-electron or statistical densities capture the bulk of the RHF radial distribution.

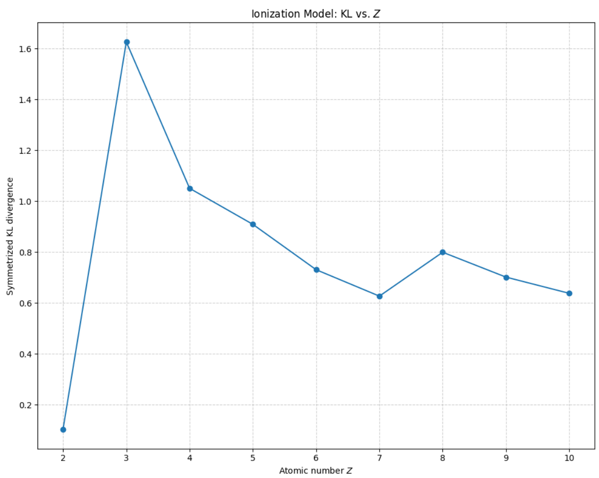


(a) KL divergence (ionization model)

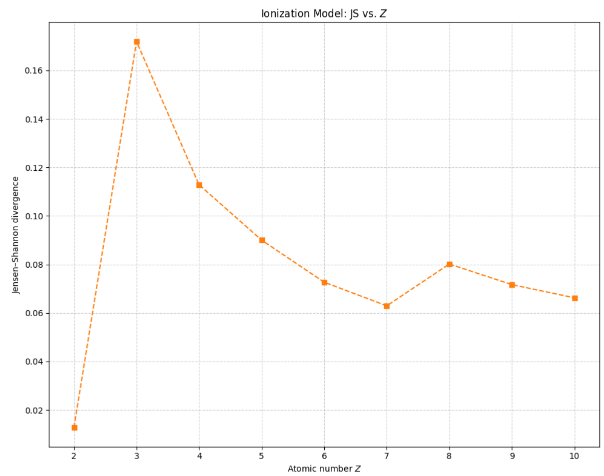


(b) JS divergence (ionization model)

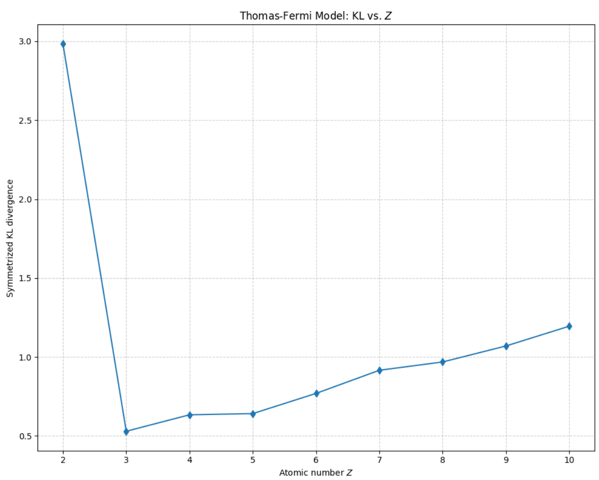


(c) KL divergence (Thomas–Fermi model)

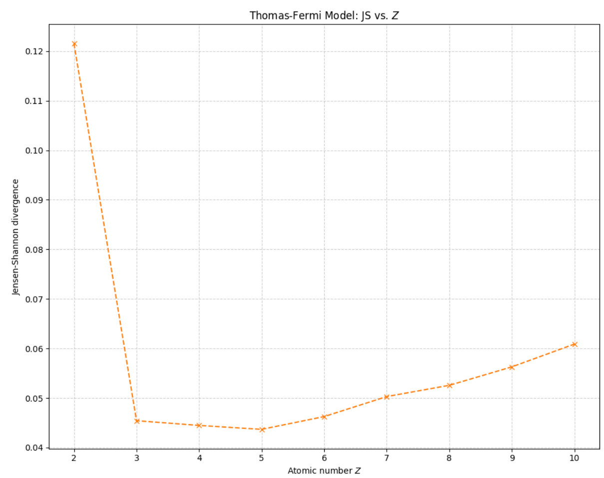


(d) JS divergence (Thomas–Fermi model)

Figure 3: Information-theoretic divergences for the two reference densities. (a,b) Ionization-model KL and JS. (c,d) Thomas–Fermi-model KL and JS.

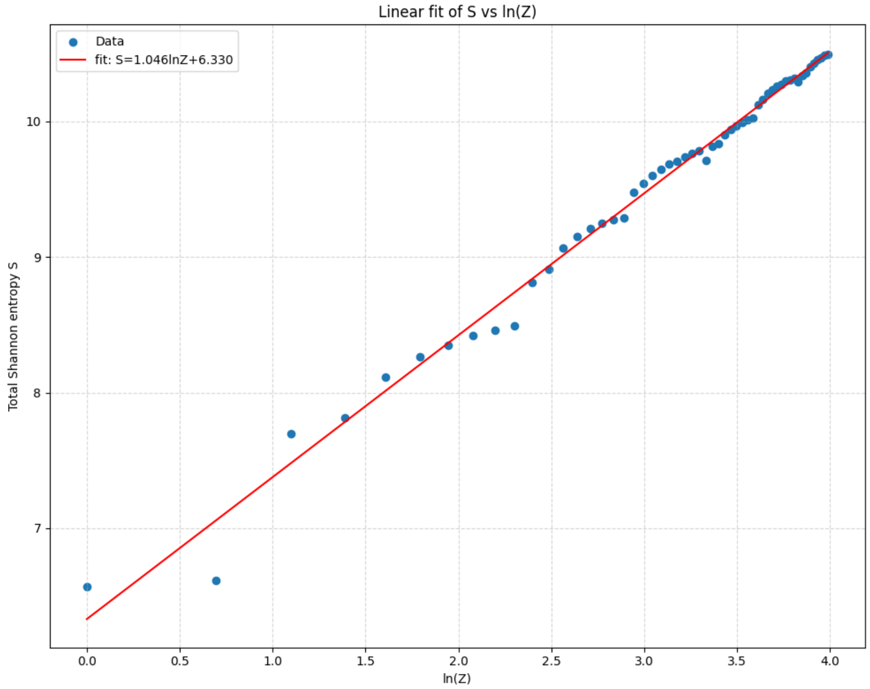


Figure 4: Total Shannon entropy $S$ plotted against $\ln Z$, with a linear fit
$S \approx 1.046 \ln(Z) + 6.330, \quad R^2 = 0.9895.$

The nearly perfect $R^2$ demonstrates that across many $Z$ values the total entropy grows logarithmically with nuclear charge $Z$.

## Summary

We have carried out a systematic information-theoretic analysis of the second-period atoms (He–Ne) in their RHF ground states. These results demonstrate that atomic information content grows in a simple, predictable way with nuclear charge, and that RHF densities remain close to classical reference models in an information-theoretic sense.

## Computational Resources & Libraries

All code was written in Python using the following libraries:

- numpy
- matplotlib
- scipy

The computations were performed on a system with an Intel® Core™ i7-8750H CPU @ 2.20 GHz and 16 GB of DDR4 RAM.

## References


[1] C. E. Shannon, *A Mathematical Theory of Communication*, Bell System Technical Journal **27**, 379–423 (1948).

[2] C. F. Bunge and J. A. Barrientos, *Hartree–Fock Ground-State Atomic Wave Functions Expanded in Slater-Type Orbitals*, At. Data Nucl. Data Tables **53**(1), 113–162 (1993).

[3] Ch. C. Moustakidis, K. Ch. Chatzisavvas, and C. P. Panos, *Information entropy, information distances, and complexity in atoms*, Phys. Rev. A **72**, 032514 (2005).